Meteorology and Atmospheric Physics (2022) 134:96
https://doi.org/10.1007/s00703-022-00932-3

ORIGINAL PAPER

Changes in tropospheric ozone concentration over Indo-Gangetic Plains: the role of meteorological parameters

Swagata Payra[1] · Priyanshu Gupta[2] · Abhijit Sarkar[3] · R. Bhatla[4,5] · Sunita Verma[2,5]

Received: 10 February 2022 / Accepted: 20 September 2022 / Published online: 12 October 2022
© The Author(s), under exclusive licence to Springer-Verlag GmbH Austria, part of Springer Nature 2022

Abstract

This study seeks to understand and quantify the changes in tropospheric ozone (O_3) in lower troposphere (LT), middle troposphere (MT) and upper middle troposphere (UMT) over the Indo-Gangetic Plains (IGPs), India during the COVID-19 lockdown 2020 with that of pre-lockdown 2019. The gridded datasets of ozone from the European Centre for Medium-range Weather Forecasts (ECMWF) reanalysis product, ERA5 in combination with statistical interpolated (IDWs) surface NO_2 observations, present a consistent picture and indicate a significant tropospheric ozone enhancement over IGP during COVID-19 lockdown restrictions in May 2020. The Paper also examines the influencing role of meteorological parameters on increasing ozone concentration. Over LT, an increase in O_3 concentration (23%) is observed and in MT to UMT an enhancement of about 9–18% in O_3 concentration have been seen during May 2020 with respect to May 2019. An investigation on causes of increasing ozone concentration (35–85 ppbv) from MT to UMT during May 2020 reveals that there was significant rise (by 1–6%) in low cloud cover (LCC). Notably, higher LCC increases the backscattering of upward solar radiation from the top of the atmosphere. A positive difference of 5–25 W/m^2 in upward solar radiation (USR) is observed across the entire study region. The result suggests that higher LCC significantly contributed to the enhanced USR. Thereby, resulting in higher photolysis rate that lead to an increase in mid tropospheric ozone concentration during May 2020. The results highlight the importance of LCC as an important pathway in ozone formation and aid in scientific understanding of it.

1 Introduction

Alongside the extensive developmental activities taking place across the country, air quality emerged as the most life-threatening challenge in India, particularly in cities with level of air pollutants often exceeding the National Ambient Air Quality Standards (NAAQS) (Guttikunda et al. 2014). With the end of 2019, one of the worst global catastrophes has dawned upon humanity in the form of zoonotic contagious virus named severe acute respiratory syndrome coronavirus 2 (SARS-CoV-2) (Lai et al. 2020). With its origins in Wuhan, China; the virus spread rapidly across the world within a mere time period of approximately 3 months and the disease was declared as pandemic by the World Health Organization on 11th March, 2020 (WHO 2020). The outbreak of COVID-19 (coronavirus disease 2019) started in the late 2019 and is still an ongoing pandemic event. To combat this deadly coronavirus disease all trains, automobiles, industries and factories came to halt, bringing down the pollution level of most polluted cities and making the sky clearly visible and clean.

Interestingly, halting major anthropogenic activities in large geographical regions, to arrest further spread of COVID-19 seems to serve certain inadvertent benefits in terms of improving air quality. Various scientific studies have reported the air quality index of most Indian cities during lockdown period. Sharma et al. (2020) observed the air quality by measuring six criteria pollutants over 20 cities of

Responsible Editor: Silvia Trini Castelli.

✉ Sunita Verma
verma.sunita@gmail.com

[1] Department of Remote Sensing, Birla Institute of Technology Mesra, Ranchi, Jharkhand, India

[2] Institute of Environment and Sustainable Development, Banaras Hindu University, Varanasi, Uttar Pradesh, India

[3] National Centre for Medium Range Weather Forecasting, Ministry of Earth Sciences, Noida, Uttar Pradesh, India

[4] Department of Geophysics, Banaras Hindu University, Varanasi, Uttar Pradesh, India

[5] DST-Mahamana Centre of Excellence in Climate Change Research, Banaras Hindu University, Varanasi, Uttar Pradesh, India

India from 16th March to 14th April of 2017 to 2020 and found maximum reduction in $PM_{2.5}$ concentrations in most of the cities and increase in O_3 level that may be due to decrease in $PM_{2.5}$ and NO_x. A significant decrease in aerosol loading is also observed over most parts of India; especially northern India experienced a drop-in aerosol optical depth (AOD) concentration during 31st March to 5th April 2020 as compared to same period of the previous years (Soni et al. 2021). Ratnam et al. (2021), also reported the decrease in AOD over Central India during lockdown 2020.

Though nationwide lockdown reported a sharp decline of pollutants (PM, NO_2, CO, AOD) concentration, but increasing ozone concentration caught the public's attention. Sulaymon et al (2021) reported reduction in NO_2 (50.6%), CO (16.6%), $PM_{2.5}$ (41.2%) and PM_{10} (33.1%), while increment in O_3 concentration (149%) over Wuhan, China during COVID-19. Previous studies suggest that increase in surface O_3 concentration may arise due to reduced NO_2, $PM_{2.5}$ and PM_{10} levels (Liu et al. 2013; Li et al. 2017).

O_3 is a secondary pollutant that forms in the presence of sunlight and its precursors viz, nitrogen oxides (NO_x), and volatile organic compounds (VOCs). It is produced by an intricate photochemical reaction, taking place in the presence of sunlight between nitrogen oxides ($NO_x = NO + NO_2$) and volatile organic compounds (VOCs). Its formation and destruction are regulated by the natural phenomena like photolytic destruction of the ozone and also affected by human interference. Its concentration depends on photochemistry, physical/chemical removal and transport over local, regional, and global scales (Lal et al. 2000). The long-range transport can influence the ozone and other pollutant concentration both in rural and urban environments (Satheesh Chandran et al. 2021; Jain et al. 2022). It is greatly influenced by predominant meteorological conditions (temperature, solar flux, wind speed and relative humidity). Several authors have studied the possible interaction of surface temperature and cloud cover on ozone concentration (Liu et al. 2006; Voulgarakis et al. 2009; Jana et al. 2010, 2011; Midya et al. 2011; Ghosh et al. 2015). O_3 concentration increases with an increase in solar flux and temperature (Gorai et al. 2015). Relative to clear sky conditions, presence of cloud decreases the net chemical production of ozone at the surface by 15% and increases in upper troposphere by 15% (Wild et al. 2000). Singh et al. (2020) showed almost constant trends in ozone with some fluctuations for all the regions except in the IGPs sites. Earlier studies have reported that the meteorological parameters can affect and bring substantial changes in O_3 and NO_2 concentration (Zhao et al. 2020; Nie et al. 2021; Kumar et al. 2022). Miyazak et al. (2021) have reported 15% and 18–25% reduction in anthropogenic NO_x emissions on global and regional level in April–May 2020. Kumar et al. (2022) found an increase in O_3 (~ 15–20%) concentration over central and IGP region.

Additionally, there are different reasons for the ozone changes in the upper troposphere. For example, the study made by Hemanth Kumar et al. (2018) using MST radar vertical wind and balloon borne ECC ozone sondes over South India monsoon region revealed that the strong updrafts during deep convection are also responsible for the vertical transport of ozone from lower troposphere to upper troposphere. Moreover, May is the month when frequent intrusions occur from stratosphere which might also bring ozone rich air into the upper troposphere.

However, the reason for rise in vertical distribution of tropospheric O_3 concentration, despite a large reduction in emissions is still unknown, necessitating further research to better understand the processes that lead to an increase of tropospheric ozone.

Therefore, present study has been focused to investigate the vertical distribution of the tropospheric O_3 with special focus on LT, MT, UMT region during the COVID-19 induced lockdown in May 2020 with respect to previous normal year of May 2019 and average of 2015–2019 year over IGPs, India. The main objective of the present study is to understand and quantify the changes in the vertical distribution of O_3 over the IGP region during the lockdown. First, we have analyzed the spatiotemporal variations of ozone concentration of ERA5 in lower troposphere (LT) i.e. (1000–850 hPa) and further proceeded with meteorological factors like; MERRA-2 surface temperature. The NO_2 and O_3 are investigated from the perspective of atmospheric chemistry (Bozem et al. 2017). Then, the impact of LCC on MT and UMT ozone (850–400 hPa) are explored to investigate changes in the various amount of downward solar radiation (DSR), outgoing longwave radiation (OLR) and upward solar radiation (USR).

The organization of the paper is as follows: Sect. 2 describes the study area; Sect. 3 presents the methodology and data description. Section 4 discusses the spatiotemporal variations of ozone concentration obtained from ECMWF reanalysis product ERA5, in combination with continuous geo-statistical interpolation surface pollutants NO_2 observations with meteorological factors like; MERRA-2 surface temperature. The impact of LCC on tropospheric ozone, and surface temperature are explored in details. The amount of DSR, OLR and USR that is attenuated and backscattered when low clouds are present is also explored. Finally, the conclusion is drawn in Sect. 5.

2 Study area

The study consists of Indo-Gangetic Plains (20°30′–32°48 ′N and 72°54′–90°0 ′E), which lies toward the foothills of Himalaya, stretching from the Thar deserts in the west to eastern part of India (Fig. 1). It is socially significant,

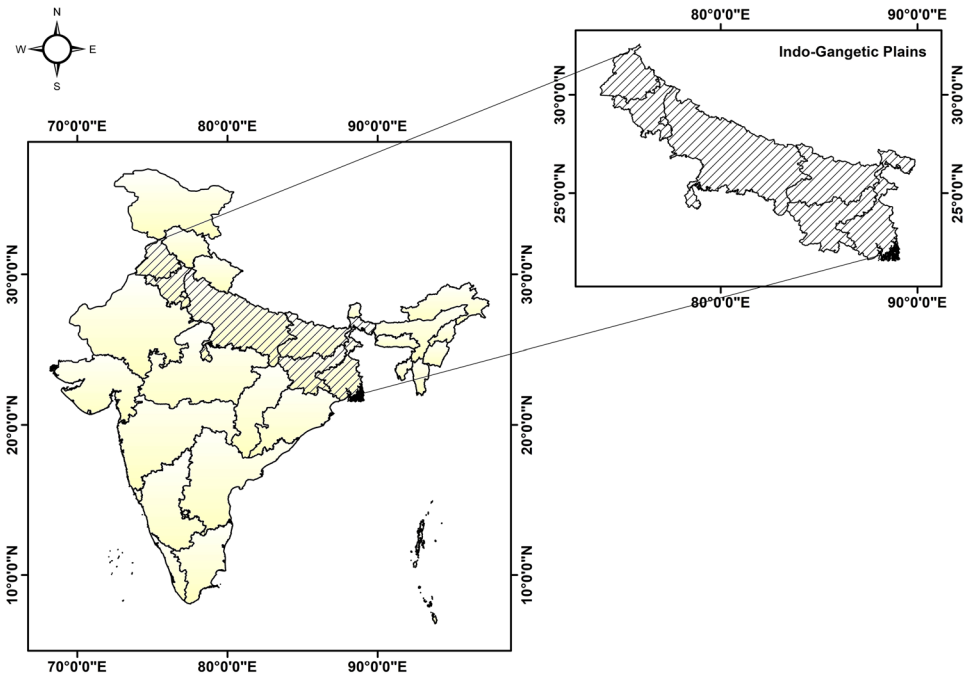

Fig. 1 Geographical location of Indo-Gangetic Plains on India map

economically strategic and an environmentally sensitive domain of India. According to Timsina and Connor (2001) region experiences the subtropical to warm temperate climate, distinguished by dry and cool winters and wet to warm summers. IGPs are considered as the aerosol laden, agriculturally productive and densely populated areas (Kishcha et al. 2011), with high intra-seasonal and intra-annual variability of pollutants (Dey and Di Girolamo 2010; Henriksson et al. 2011; Kaskaoutis et al. 2011).

3 Data and methodology

European Centre for Medium-range Weather Forecasts (ECMWF) reanalysis, ERA5 daily datasets of ozone mixing ratio (ppbv) at 0.25° × 0.25° grid resolution is used to analyze the spatiotemporal variation of ozone, over the IGPs region. LCC datasets are also derived from ERA5. OLR, DSR and USR data have been collected from NCEP NCAR reanalysis product. MERRA-2 monthly dataset of surface Temperature (2 m) at 0.5° × 0.625° grid resolution is used for temperature analysis. Surface NO_2 for different stations; Varanasi, Delhi, Kolkata, Amritsar, Agra, Lucknow, Bulandshahr, Ghaziabad, Noida, Gaya and Siliguri have been acquired from Central Pollution Control Board (CPCB) site. Their respective latitude and longitude have been given in Table 1 of Annexure 1. Further these stations are used to create spatial plot for surface NO_2 using inverse distance weighted (IDW) interpolation method.

3.1 Inverse distance weighting (IDW)

IDW is most popular spatial interpolation method to assess an unknown value at a location using some known values with corresponding weighted values (Lu and Wong 2008). IDW is quite popular for its simplicity, processing speed, and capacity to handle dispersed data. It implicates the process of allocating values to unknown points with a scattered set of known points. This paper has used the IDW techniques for spatial NO_2 data interpolation, which is based on the ideas of distance weighting. It helps to estimate the unknown spatial NO_2 data from known NO_2 station data.

The inverse distance weighting was calculated using the following formula:

$$NO_{2(P)} = \sum_{i=1}^{n} w_i NO_{2(i)}$$

$$w_i = \frac{d_i^{-x}}{\sum_{i=1}^{n} d_i^{-x}}$$

where, $NO_{2(P)}$ is point value to be estimated i.e., unknown NO_2 (μg/m^3) data, whereas $NO_{2(i)}$ is the known NO_2 values at *i*th point i.e., NO_2 data of known surface NO_2 stations. *n* is the total number of points of NO_2 data stations. d_i is the distance between unknown and known NO_2 value for *i*th point, *x* means the power, and is also a control parameter.

3.2 ERA5

ERA5 is fifth generation ECMWF reanalysis product. Data are available from 1950, split into climate data store entries for 1950–1978 and from 1979 onwards. It is created using 4D-Var data assimilation and model forecasts in cycle 41R2 (CY41R2) within integrated forecast system (IFS) of ECMWF. ERA5 provides different variables of cloud cover properties. In this study, we have used ERA5 low cloud cover and ozone datasets. Low cloud is a single level field incorporated from surface to 2 km atmospheric altitude (approx. 850 hPa). ERA5 ozone mixing ratio is produced by an updated version of the ozone parameterization of Cariolle and Deque (1986) scheme as described by Cariolle and Teyssèdre (2007). Moreover, tropospheric ozone reanalysis has been also evaluated by Park et al. (2020) over East Asia. Evaluation of tropospheric ozone reanalysis with independent ozonesonde observations in East Asia. ERA5 provided ozone mixing ratio datasets at 37 pressure levels from the surface to 1 hPa with spatial resolution of ($0.25° \times 0.25°$). To derive ozone profiles, the ERA-5 reanalysis model assimilates several ozone satellite products as explained by Hersbach et al. (2020). Several authors have also evaluated the recently launched ERA-5 ozone datasets in troposphere, stratosphere and polar regions. (Shangguan et al. 2019; Bernet et al. 2021; Wang et al. 2021).

3.3 MERRA-2

The assimilated product of MERRA-2 developed at NASA's Global Modelling and Assimilation Office (GMAO) spanning the time period from 1980 to the present (Gelaro et al. 2017). It provides gridded data at $0.5° \times 0.625°$ grid resolution between the surface and 0.01 hPa at 72 sigma-pressure hybrid levels. MERRA to MERRA-2 updated version is described in details by Molod et al. (2015). The observing system update includes latest satellite data. The Infrared Atmospheric Sounding Interferometer (IASI) started in September 2008. The Advanced Technology Microwave Sounder, worked on Soumi, NPOESS Preparatory Program (NPP) starting in November 2011. The Cross-Track Infrared sounder used in Soumi NPP satellite working since April 2012. In MERRA-2 stratospheric sounding units retrieved radiance data are used with a more advanced community radiative transfer model. McCarty et al. (2016) gave a detailed comprehensive description of MERRA-2. In this study we have used (M2TMNXSLVv5.12.4) product for surface temperature. The MERRA-2 surface temperature has also been validated previously over Indian regions (Gupta et al. 2020).

4 Result and discussions

Indo-Gangetic Plains (IGPs) region in India act as global hotspot in terms of pollutant loading. In consecutive sections, we have analyzed the spatiotemporal variations of surface ozone concentration in lower troposphere (LT) i.e. (1000–850 hPa). The NO_2 and O_3 are investigated from the perspective of atmospheric chemistry (Bozem et al. 2017). Then, we have examined the impact of LCC on mid and upper mid tropospheric ozone (850–400 hPa), and resulting changes in the various amount of downward solar radiation (DSR), outgoing longwave radiation (OLR) and upward solar radiation (USR).

4.1 Spatiotemporal variation of tropospheric ozone

Figure 2 demonstrate the averaged tropospheric ozone concentration (1000–400 hPa) retrieved from ERA5 product during the period (a) May 2019, (b) May 2020 and (c) difference of these two values. A decreasing pattern of ozone from upper to lower IGPs (Fig. 2a) is observed i.e., upper region recorded high ozone (35–42 ppbv) that significantly decreased towards central (33–40 ppbv) and lower region (< 35 ppbv) during May 2019. On the other hand, in May 2020 higher (Fig. 2b) ozone (32–42 ppbv) values were found over the entire IGPs region with the similar trend. During 2020, ozone concentration of 40–42 ppbv is observed

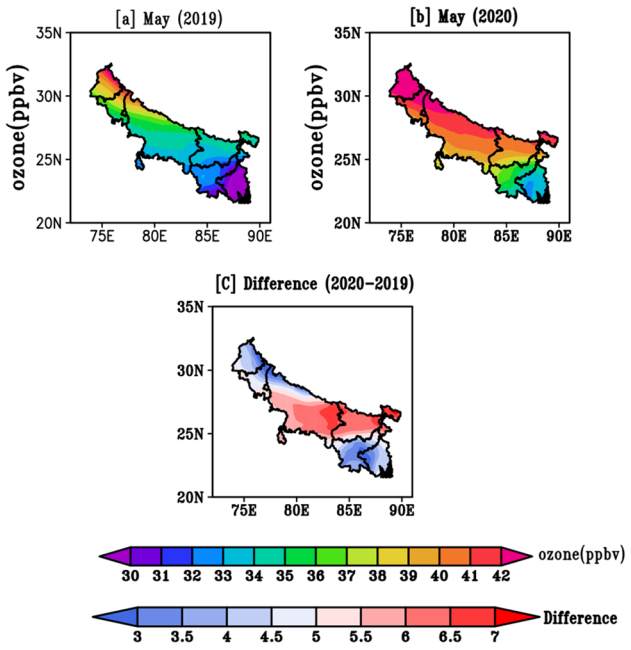

Fig. 2 Ozone concentration (1000–400 hpa) retrieved from ERA5 product over IGPs region during the period **a** May 2019, **b** May 2020 and **c** difference (2020–2019)

towards upper IGPs, while around 37–42 ppbv are seen over central and a minimum towards lower IGPs (32–37 ppbv) region. Overall, relative to the previous year, May 2020 shows high tropospheric ozone with a positive difference of 3–7 ppbv (Fig. 2c).

4.2 Variation in surface NO_2

Spatial variations in mean surface NO_2 during May 2019 and May 2020 for IGPs, India are shown in Fig. 3. Comparatively, May 2019 reflects high surface NO_2 ($\mu g/m^3$) concentration throughout the IGPs region. In upper IGPs, NO_2 in the range of 15–40 $\mu g/m^3$ observed, which became maximum 40–75 $\mu g/m^3$ in middle and decreased in lower region (~ 10–35 $\mu g/m^3$). In May 2020, low concentration (10–40 $\mu g/m^3$) of surface NO_2 was observed throughout the IGPs region. This is due to government imposed complete lockdown (2020) which restricted the transportation and industrial activities which lead to notable decrease in surface pollutants particularly, NO_2 concentrations. Since surface O_3 and NO_x are chemically coupled, reducing NO_x emissions results in a strikingly nonlinear reaction, and each subsequent drop in nitrogen dioxide (NO_2) is inevitably accompanied by an increase in the atmospheric concentration of O_3. Reduction in surface NO_2 consequently increased the ground O_3 concentration (Liu et al. 2013; Li et al. 2017; Sulaymon et al. 2021).

4.3 Vertical distribution of ozone

Vertical distribution of ozone concentration retrieved from ERA-5 reanalysis product during pre-lockdown (2015–2019, May), lockdown (2020, May) and post-lockdown (2021, May) period averaged over the IGPs region is shown in Fig. 4. Compared to previous and later period, in May 2020 high ozone concentration is seen from surface to upper troposphere. This increase in lower tropospheric (LT) ozone concentration might have occurred due to decline in NO_2 as shown in Fig. 3. Sharma et al. (2020) also concluded that the average of CO, NO_2, $PM_{2.5}$ and PM_{10}, was decreased by

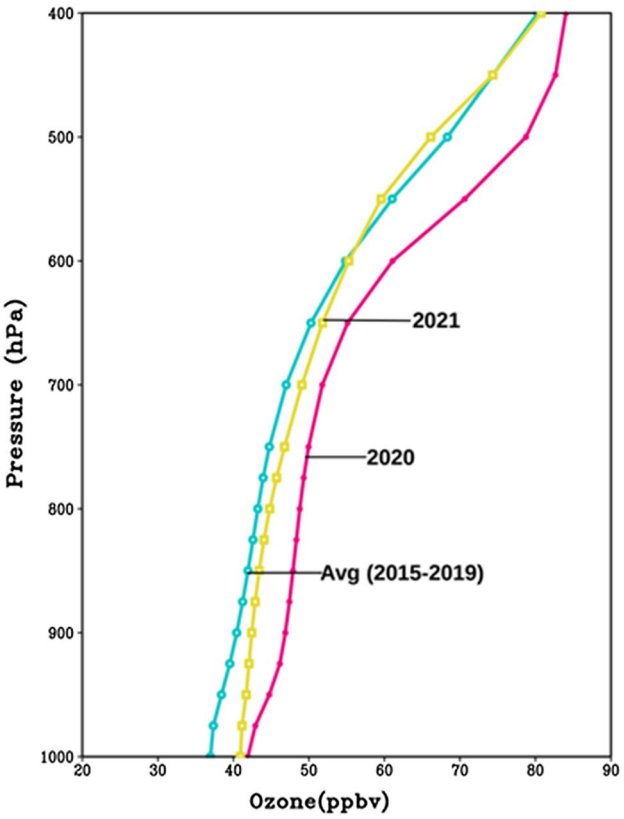

Fig. 4 Vertical ozone profile retrieved from ERA5 reanalysis datasets for prelockdown, avg. (2015–2019), lockdown (2020) and post-lockdown (2021) period

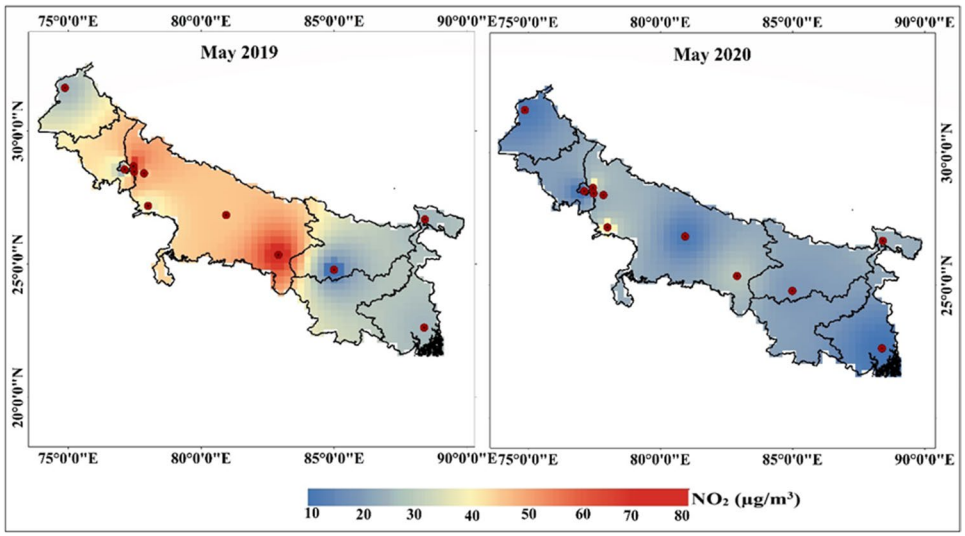

Fig. 3 Monthly average NO_2 variations for the period May 2019 and May 2020

10%, 18%, 43% and 31%, respectively, and a 17% increase in O_3 concentration was observed during lockdown compared with pre-lockdown period over India. Further a significant rise in ozone concentration (58–85 ppbv) is observed from mid to upper tropospheric 600 to 400 hPa pressure level. To explore the reason of the increase, we have further explored the variations in temperature, OLR, DSR, USR and LCC profiles over the study period and region.

4.4 Spatiotemporal variation of temperature

Figure 5 shows the spatial distribution of surface temperature (°C) retrieved from MERRA-2 over IGP, India. In comparison with previous year, lockdown period reveals a significant decrease in surface mean temperature due to less solar insolation reaching at earth surface. During May 2019 (Fig. 5a), temperature within the range of 26–35 °C is reached with maximum temperature lying towards the central IGPs region (31–35 °C). Figure 5b shows a further decrease in temperature in May 2020. A negative difference (−5 to −1 °C) in surface mean temperature between recent and previous year has been attained (Fig. 5c) across the entire IGPs region. This temperature reduction may be due to attenuation of solar insolation arriving at earth surface as LCC plays a crucial role in diminishing solar insolation. LCC is a part of sky covered by clouds with base height around 2 km; it primarily reflects the solar radiation and cools the Earth's surface resulting in a decrease in Earth surface temperature.

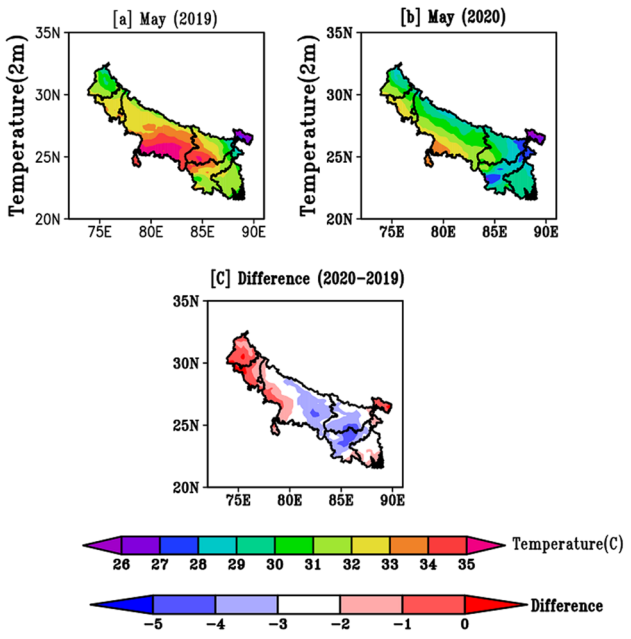

Fig. 5 Spatiotemporal variations of surface mean temperature (°C) of **a** May 2019, **b** May 2020 and **c** difference of both (2020–2019)

An inverse relation between cloudiness and temperature is found which varies drastically from 2019 to 2020. In May 2020, abundance of LCC is strongly associated with lower temperature in IGPs region, owing to cloud effects on solar insolation loss at the surface. The details are presented in Sect. 4.5. Chowdhuri et al. (2021) have also shown decreasing trends of maximum, mean and minimum temperatures from March to April 2020 (lockdown period in 2020). Comparison with 1980–2019 average, they have found a decrease in maximum (2 °C), minimum (1 °C) and mean temperature (1.5 °C) for April 2020.

4.5 Surface downward solar radiation flux and outgoing longwave radiation

Further, we have analyzed downward solar radiation flux (DSR) over the study area. DSR is the total amount of solar radiation i.e. both direct and diffuse radiations that reaches the earth surface.

Figure 6 shows the DSR at surface retrieved from NCEP/NCAR reanalysis product for the month of (a) May 2019 and (b) May 2020 over IGPs region. As shown in Fig. 6I, during May 2019, solar radiation of 270–350 W/m^2 reached the earth surface, which significantly reduced in May 2020 with a difference of −40 to −5 W/m^2. Cloud cover is one of the strongest atmospheric constituents and thus act as a strongest modulator of solar radiation energy i.e., absorbed by earth atmospheric systems and causes profound effects on DSR. Wang et al. (2019) reported maximum attenuation of DSR with attenuation ratio of 7.4% at 1200 LST. These attenuation differences are expected due to degree of pollution, solar angle differences, cloud cover and pollutant components etc. They have also mentioned that diurnal variation of DSR and their discontinuity is impacted by higher aerosol concentration and larger cloud cover.

Outgoing longwave radiation (OLR) is also analyzed in connection to verify the low temperature at 2020 and shown in Fig. 6II. OLR estimates the amount of energy emitted by the earth's surface to space. It is frequently affected by cloud cover, near surface temperature, atmospheric temperature and water vapor (Schmetz and Liu 1988). Like DSR, the decreasing pattern in OLR is also found from 2019 to 2020 with a negative difference of −13 to −5 W/m^2. Since less downward solar flux reached and absorbed by the earth surface in May 2020 there was reduction in upward longwave radiation emitted by the earth surface and atmosphere. Presence of cloud cover may trap these outgoing longwave radiations and change their pattern. According to Kyle et al. (1995) the total cloud cover and OLR are negatively correlated.

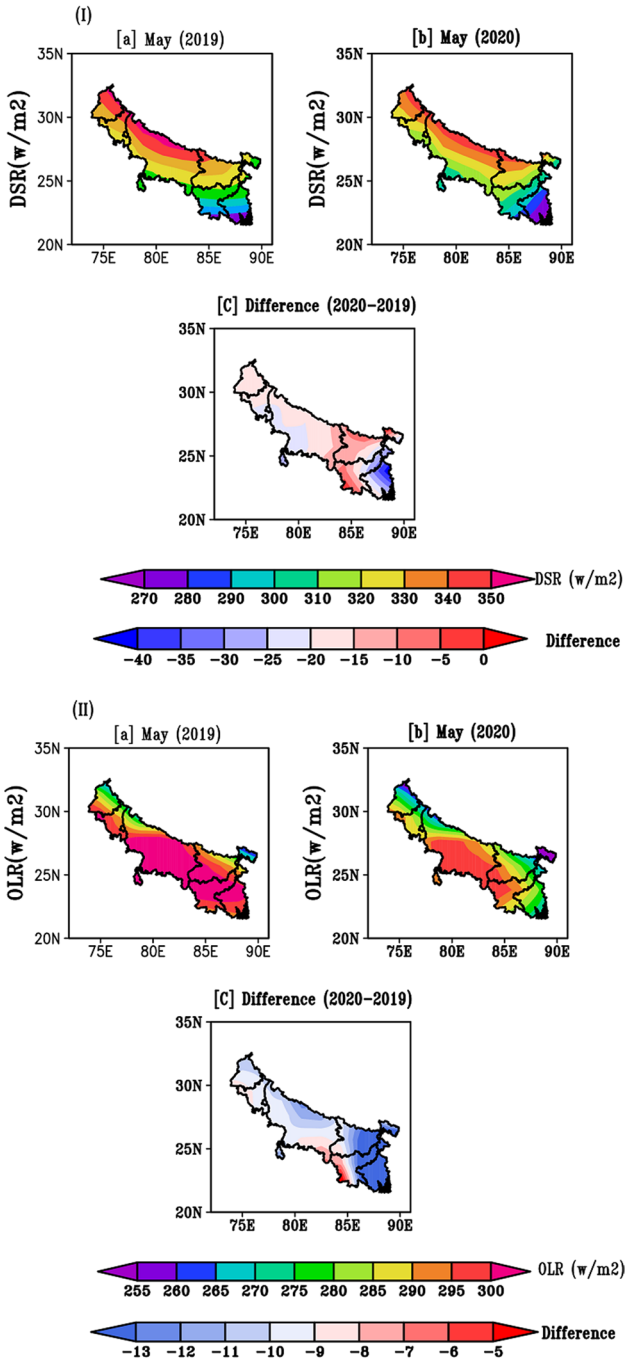

Fig. 6 Solar radiation flux retrieved from NCEP-NCAR datasets for the period **a** May 2019, **b** May 2020 and **c** difference over IGPs region. **I** Downward solar radiation flux. **II** Outgoing longwave radiation

4.6 Upward solar radiation flux at nominal top of the atmosphere

After observing the low solar insolation reaching at earth surface, we have further analyzed upward solar radiation flux at the nominal top of the atmosphere (shown in Fig. 7).

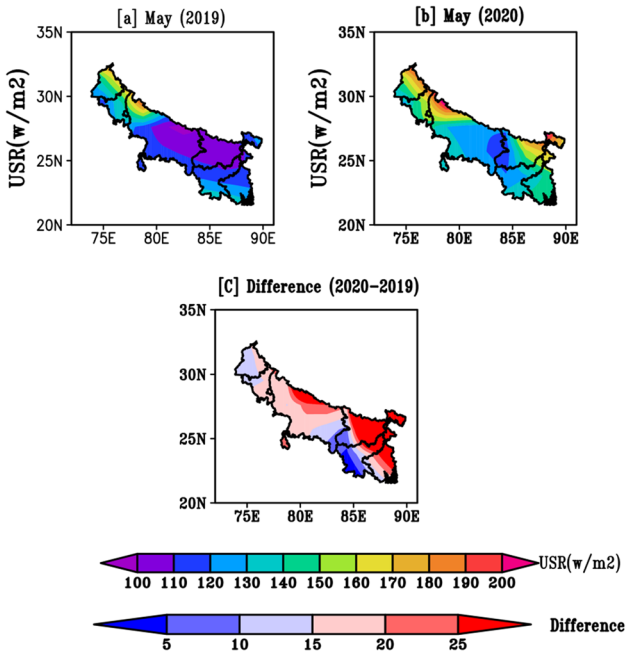

Fig. 7 Upward solar radiation flux retrieved from NCEP-NCAR over IGPs region for period **a** May 2019, **b** May 2020, **c** difference (2020–2019)

Figure 7 shows USR (top of the atmosphere) derived from NCEP/NCAR reanalysis product over IGPs region during the period (a) May 2019, (b) May 2020 and (c) the difference of these two values (2020–2019). In relation with previous years, an increase in USR has been observed in the year 2020. In May 2019, it ranges from 100 to 180 W/m^2 which significantly increases to 110–200 W/m^2 in May 2020. Increase in USR is observed specially over central and lower IGPs region. A positive difference of 5–25 W/m^2 was recorded across the entire IGPs region.

4.7 Low cloud cover

Cloud cover plays an important role in earth radiation balance. The ERA-5 cloud cover datasets is used in present analysis to understand LCC occurrence and impact on surface solar insolation, DSR, OLR and USR.

Spatial pattern of LCC during (a) May 2019, (b) May 2020 and (c) difference of these values (2020–2019) are shown in Fig. 8. LCC within the range of 1–23% are found in May 2019, and it increased in 2020 by a positive difference of 1–6%. Presence of high LCC can influence solar radiation by backscattering larger amount of incoming downward solar radiation which led to enhanced upward solar radiation flux. Increase of USR at the top of atmosphere might have intensified the ozone formation reaction and as a consequence, columnar ozone concentration has increased.

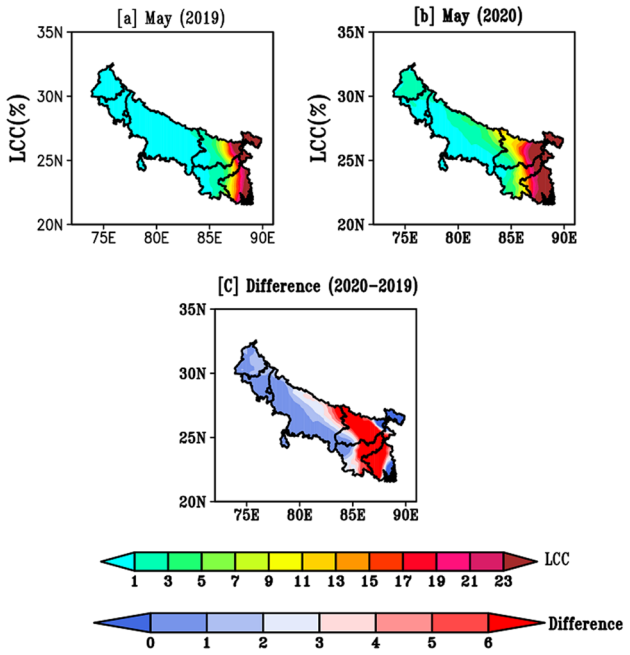

Fig. 8 Spatial variations of low cloud cover (%) over IGPs region are shown for **a** May 2019, **b** May 2020, **c** difference (2020–2019)

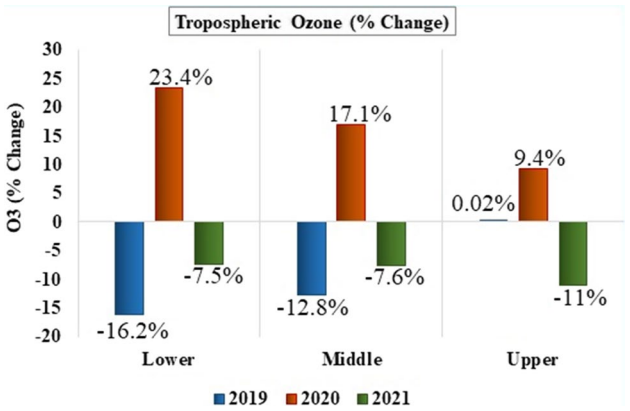

Fig. 9 Ozone (% change) for the lower, middle and upper troposhere for the period of May 2019, 2020 and 2021

4.8 Vertical distribution of ozone for annual percentage change

The ERA-5 ozone has been used to understand the impact of lockdown on the LT (1000–850 hPa), MT (850–600 hPa) and UMT (600–400 hPa) ozone concentration. Figure 9 shows the percentage change of O_3 at different levels during May 2020 (lockdown), May 2019 (pre-lockdown) and May 2021 (post-lockdown) period. Increase in ozone over LT, MT and UMT have been observed during the lockdown period compared to pre-lockdown period. A clear enhancement in vertical distribution of tropospheric O_3 concentration (~9–23%) have been noticed during 2020 (Fig. 9). Over LT, an increase in O_3 concentration (23%) is found whereas in MT to UMT (850–400 hPa), an enhancement of about 18–9% in O_3 concentration has been noticed during lockdown in May 2020 with respect to previous normal year of May 2019 over IGPs, India. Evidently, the NO_2 surface emissions reduction is found over IGP as shown in Fig. 3. The NO_2 reduction have consequently resulted in higher ozone at LT over the IGP as explained in Liu et al. (2013), Li et al. (2017), Sulaymon et al. (2021). Many studies have also shown reduction in NO_2 levels, mostly due to reductions in traffic-related emissions (Petetin et al. 2020; Siciliano et al. 2020). Keller et al. (2021) have found 18% reductions in NO_2 concentrations from February onward and 50% increase in daily mean O_3 due to non-linear atmospheric chemistry. In Spain, traffic-related emission reductions consequently lead to 51% reduction in NO_2 thereby 50% increase of O_3 concentration, possibly due to reduction in the O_3 titration by NO (Sicard et al. 2020). Similarly, decrease in NO_2 and increase in O_3 due to non-linear chemical effects observed by Menut et al. (2020).

An enhancement of ~1–6% in LCC is observed over MT region suggesting that the dynamical aspects of LCC might have played a key role on the observed increase in the ozone in MT and UMT over IGP regions. The presence of high LCC in May 2020 enhanced the backscattering of upward solar radiation to the top of atmosphere and corroborated well to the enhancement of the ozone formation and increment of columnar ozone concentration during lockdown period of May 2020. Tong et al. (2017) found positive correlation of solar radiation with O_3 concentration.

Thus, the increase in MT and UMT ozone concentration above the cloud is due to backscattering of solar radiation and consequent increase in photolysis rate (Liu et al. 2006). Voulgarakis et al. (2009) explained that increase of ozone in UT are caused by higher production rate due to back scattering of radiations and consequent increase in photolysis rates. Also, increased backscattered radiations by the cloud cover raise the concentration of OH radicals that leads to ozone building processes. Enhancement of the photolysis rates of ozone formations due to the backscattered solar radiations by clouds was also noted by Jana et al. (2011).

5 Conclusions

The current work examines the changes in ozone across the troposphere (1000–400 hpa) during lockdown period over IGPs India. Analysis found an increasing pattern of ozone concentration in May 2020

contrary to similar period of 2019. Further, pollutants and possible meteorological factors responsible for increasing surface and tropospheric ozone concentration have been investigated. Increase in surface O_3 explained by reduction in NO_2 and other pollutants emissions during lockdown period. Whereas, metrological factors, like; surface temperature from MERRA-2 indicates a decreasing pattern in May 2020 across IGPs region, and it reflects an inverse relation with cloudiness that varies drastically from May 2019 to May 2020. The surface downward solar radiation, outgoing longwave radiation showed a negative difference in May 2020 with that from May 2019. Whereas, the upward solar radiation at the top of the atmosphere shows an increasing pattern with a positive difference of 5–25 W/m^2 across the entire IGPs region. The cloud cover pattern reveals that LCC during May 2020 was relatively higher than that in May 2019. The increase in low cloud cover in May 2020 thus contributed to more backscattering of upward solar radiation at the top of atmosphere that resulted in enhancing the UMT ozone.

Finally, this study emphasizes two major factors that explain increase in the O_3 concentrations at lower and middle troposphere. The increase in ozone above LCC is due to an increase in backscattered solar radiation that enhances photochemical reaction and hence UMT ozone. Though surface temperature decreases due to increase in LCC, but the reduction in surface NO_2 during COVID-19 might have led to increases in the ozone concentration near the ground.

Annexure 1

See Table 1 and Fig. 10.

Table 1 Stations selected for NO_2 spatial plot using IDW techniques

Stations	Latitude	Longitude
Amritsar	31.621	74.876
New Delhi	28.628	77.241
Ghaziabad	28.685	77.453
Bulandshahr	28.407	77.849
Noida	28.569	77.393
Agra	27.169	78.936
Lucknow	26.845	80.936
Varanasi	25.350	82.908
Gaya	24.762	84.982
Kolkata	22.060	88.109
Siliguri	26.688	88.412

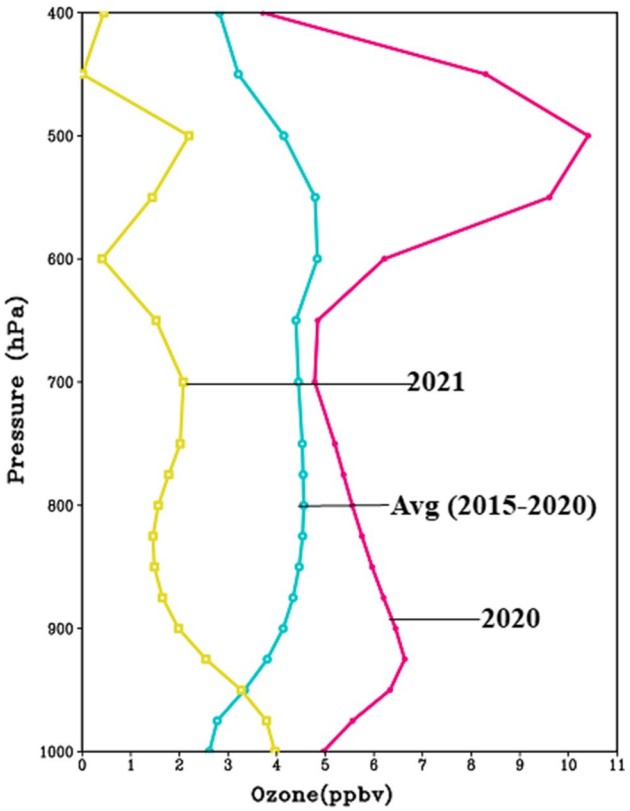

Fig. 10 Vertical profile of ozone standard deviation for pre-lockdown i.e. avg (2015–2019), lockdown (2020) and post-lockdown (2021)

Acknowledgements The authors would like to thanks the NCEP NCAR for freely providing data at https://psl.noaa.gov/data/gridded/data.ncep.reanalysis.surfaceflux.html. The first author would also like to thanks funding support under MoES (MoES/16/18/2017-RDEAS) project.

Author contributions The paper is conceptualised by SP. Material preparation, data collection and analysis were performed by PG. The paper review carried by AS. Overall, paper was supervised by SV and RB. Each author had participated sufficiently in the work to take public responsibility for appropriate portions of the content. All authors read and approved the final manuscript.

Data availability The data sets generated/analyzed during the current study are available from https://www.ecmwf.int/en/forecasts/datasets/reanalysis-datasets/era5, https://gmao.gsfc.nasa.gov/reanalysis/MERRA-2/ and https://psl.noaa.gov/data/gridded/data.ncep.reanalysis.html.

Declarations

Conflict of interest The authors declare that they have no known competing financial interest or personal relationships that could have appeared to influence the work reported in this paper.

References

Bernet L, Boyd I, Nedoluha G, Querel R, Swart D, Hocke K (2021) Validation and trend analysis of stratospheric ozone data from ground-based observations at Lauder, New Zealand. Remote Sens 13:109. https://doi.org/10.3390/rs13010109

Bozem H, Butler TM, Lawrence MG, Harder H, Martinez M, Kubistin D, Lelieveld J, Fischer H (2017) Chemical processes related to net ozone tendencies in the free troposphere. Atmos Chem Phys 17:10565–10582. https://doi.org/10.5194/acp-17-10565-2017

Cariolle D, Déqué M (1986) Southern hemisphere medium-scale waves and total ozone disturbances in a spectral general circulation model. J Geophys Res Atmos 91:10825–10846. https://doi.org/10.1029/JD091iD10p10825

Cariolle D, Teyssedre H (2007) A revised linear ozone photochemistry parameterization for use in transport and general circulation models: multi-annual simulations. Atmos Chem Phys 7:2183–2196. https://doi.org/10.5194/acp-7-2183-2007

Chowdhuri I et al (2021) Have any effect of COVID-19 lockdown on environmental sustainability? A study from most polluted metropolitan area of India. Stoch Environ Res Risk Assess. https://doi.org/10.1007/s00477-021-02019-8

Dey S, Di Girolamo L (2010) A climatology of aerosol optical and microphysical properties over the Indian subcontinent from 9 years (2000–2008) of multiangle imaging spectroradiometer (MISR) data. J Geophys Res Atmos. https://doi.org/10.1029/2009JD013395

Gelaro R et al (2017) The modern-era retrospective analysis for research and applications, version 2 (MERRA-2). J Clim 30:5419–5454. https://doi.org/10.1175/JCLI-D-16-0758.1

Ghosh D, Midya SK, Sarkar U, Mukherjee T (2015) Variability of surface ozone with cloud coverage over Kolkata, India. J Earth Syst Sci 124:303–319. https://doi.org/10.1007/s12040-015-0543-3

Gorai AK, Tuluri F, Tchounwou PB, Ambinakudige S (2015) Influence of local meteorology and NO_2 conditions on ground-level ozone concentrations in the eastern part of Texas, USA. Air Qual Atmos Health 8:81–96. https://doi.org/10.1007/s11869-014-0276-5

Gupta P et al (2020) Validation of surface temperature derived from MERRA-2 reanalysis against IMD gridded data set over India. Earth Space Sci 7:e2019EA000910

Guttikunda SK, Goel R, Pant P (2014) Nature of air pollution, emission sources, and management in the Indian cities. Atmos Environ 95:501–510. https://doi.org/10.1016/j.atmosenv.2014.07.006

Hemanth Kumar A, Venkat Ratnam M, Sunilkumar SV et al (2018) Cross tropopause flux observed at sub-daily scales over the South Indian monsoon regions. Atmos Res 201:72–85. https://doi.org/10.1016/j.atmosres.2017.10.017

Henriksson SV et al (2011) Spatial distributions and seasonal cycles of aerosols in India and China seen in global climate-aerosol model. Atmos Chem Phys 11:7975–7990. https://doi.org/10.5194/acp-11-7975-2011

Hersbach H, Bell B, Berrisford P, Hirahara S, Horányi A, Muñoz-Sabater J, Thépaut JN (2020) The ERA5 global reanalysis. Q J R Meteorol Soc 146(730):1999–2049. https://doi.org/10.1002/qj.3803

Jain CD, Ratnam MV, Madhavan BL et al (2022) Impact of regional transport on total OX ($NO_2 + O_3$) concentrations observed at a tropical rural location. Atmos Pollut Res 13:101408. https://doi.org/10.1016/j.apr.2022.101408

Jana PK, Saha DK, Midya SK (2010) Effect of cloud on atmospheric ozone formation over Kolkata (22°34′N, 88°24′E), India. Indian J Phys 84:367–375. https://doi.org/10.1007/s12648-010-0020-4

Jana PK, Saha I, Mukhopadhyay S, Sarkar D (2011) Effect of cloud on atmospheric ozone formation over Hyderabad (17.27°N, 78.28°E), India. Indian J Phys 85:1569–1580. https://doi.org/10.1007/s12648-011-0173-9

Kaskaoutis DG et al (2011) Contrasting aerosol trends over South Asia during the last decade based on MODIS observations. Atmos Meas Tech Discuss. https://doi.org/10.5194/amtd-4-5275-2011

Keller CA, Evans MJ, Knowland KE, Hasenkopf CA, Modekurty S, Lucchesi RA, Oda FBB, Mandarino FC, Díaz Suárez MV, Ryan RG (2021) Global impact of COVID-19 restrictions on the surface concentrations of nitrogen dioxide and ozone. Atmos Chem Phys 21:3555–3592. https://doi.org/10.5194/acp-21-3555-2021

Kishcha P, Starobinets B, Kalashnikova O, Alpert P (2011) Aerosol optical thickness trends and population growth in the Indian subcontinent. Int J Remote Sens 32:9137–9149. https://doi.org/10.1080/01431161.2010.550333

Kumar AH, Ratnam MV, Jain CD (2022) Influence of background dynamics on the vertical distribution of trace gases (CO/WV/O_3) in the UTLS region during COVID-19 lockdown over India. Atmos Res 265:105876. https://doi.org/10.1016/j.atmosres.2021.105876

Kyle HL, Weiss M, Ardanuy P (1995) Cloud, surface temperature, and outgoing longwave radiation for the period from 1979 to 1990. J Clim 8:2644–2658. https://doi.org/10.1175/1520-0442(1995)008%3c2644:CSTAOL%3e2.0.CO;2

Lai C-C, Shih T-P, Ko W-C, Tang H-J, Hsueh P-R (2020) Severe acute respiratory syndrome coronavirus 2 (SARS-CoV-2) and coronavirus disease-2019 (COVID-19): the epidemic and the challenges. Int J Antimicrob Agents 55:105924. https://doi.org/10.1016/j.ijantimicag.2020.105924

Lal S, Naja M, Subbaraya BH (2000) Seasonal variations in surface ozone and its precursors over an urban site in India. Atmos Environ 34:2713–2724. https://doi.org/10.1016/S1352-2310(99)00510-5

Li M et al (2017) Impacts of aerosol-radiation feedback on local air quality during a severe haze episode in Nanjing megacity, eastern China. Tellus B Chem Phys Meteorol 69:1339548

Liu H et al (2006) Radiative effect of clouds on tropospheric chemistry in a global three-dimensional chemical transport model. J Geophys Res Atmos. https://doi.org/10.1029/2005JD006403

Liu H, Wang XM, Pang JM, He KB (2013) Feasibility and difficulties of China's new air quality standard compliance: PRD case of $PM_{2.5}$ and ozone from 2010 to 2025. Atmos Chem Phys 13:12013–12027. https://doi.org/10.5194/acp-13-12013-2013

Lu GY, Wong DW (2008) An adaptive inverse-distance weighting spatial interpolation technique. Comput Geosci 34:1044–1055. https://doi.org/10.1016/j.cageo.2007.07.010

McCarty W, Coy L, Gelaro R, Merkova D, Smith EB, Sienkiewicz M, Wargan K (2016) MERRA-2 input observations: summary and assessment. NASA Tech Memo NASA/TM–2016-104606/Vol. 46, 64 pp. https://ntrs.nasa.gov/archive/nasa/casi.ntrs.nasa.gov/20160014544.pdf

Menut L, Bessagnet B, Siour G, Mailler S, Pennel R, Cholakian A (2020) Impact of lockdown measures to combat Covid-19 on air quality over western Europe. Sci Total Environ 741:140426. https://doi.org/10.1016/j.scitotenv.2020.140426

Midya SK, Ghosh D, Ganda SC, Sarkar H (2011) Seasonal variation of daily total column ozone (TCO) and role of its depletion and formation rate on surface temperature over Dumdum at Kolkata, India. Indian J Phys 85:1247

Miyazak K, Bowman K, Sekiya T, Takigawa M, Neu JL, Sudo K et al (2021) Global tropospheric ozone responses to reduced NO_x emissions linked to the COVID-19 worldwide lockdowns. Sci Adv 7:eabf7460. https://doi.org/10.1126/sciadv.abf7460

Molod A, Takacs L, Suarez M, Bacmeister J (2015) Development of the GEOS-5 atmospheric general circulation model: evolution

from MERRA to MERRA2. Geosci Model Dev 8:1339–1356. https://doi.org/10.5194/gmd-8-1339-2015
Nie D et al (2021) Changes of air quality and its associated health and economic burden in 31 provincial capital cities in China during COVID-19 pandemic. Atmos Res 249:105328. https://doi.org/10.1016/j.atmosres.2020.105328
Park S, Son SW, Jung MI, Park J, Park SS (2020) Evaluation of tropospheric ozone reanalyses with independent ozonesonde observations in East Asia. Geosci Lett 7(1):1–12
Petetin H, Bowdalo D, Soret A, Guevara M, Jorba O, Serradell K, Pérez García-Pando C (2020) Meteorology-normalized impact of the COVID-19 lockdown upon NO_2 pollution in Spain. Atmos Chem Phys 20:11119–11141. https://doi.org/10.5194/acp-20-11119-2020
Ratnam MV, Prasad P, Raj STA, Hoteit I (2021) Effect of lockdown due to COVID-19 on the aerosol and trace gases spatial distribution over India and adjoining regions. Aerosol Air Qual Res 21:1–13. https://doi.org/10.4209/aaqr.2020.07.0397
Satheesh Chandran PR, Sunilkumar SV, Muhsin M et al (2021) Effect of meteorology on the variability of ozone in the troposphere and lower stratosphere over a tropical station Thumba (8.5°N, 76.9°E). J Atmos Sol Terr Phys 215:105567. https://doi.org/10.1016/j.jastp.2021.105567
Schmetz J, Liu Q (1988) Outgoing longwave radiation and its diurnal variation at regional scales derived from Meteosat. J Geophys Res Atmos 93:11192–11204. https://doi.org/10.1029/JD093iD09p11192
Shangguan M, Wang W, Jin S (2019) Variability of temperature and ozone in the upper troposphere and lower stratosphere from multi-satellite observations and reanalysis data. Atmos Chem Phys 19:6659–6679. https://doi.org/10.5194/acp-19-6659-2019
Sharma S, Zhang M, Gao J, Zhang H, Kota SH (2020) Effect of restricted emissions during COVID-19 on air quality in India. Sci Total Environ 728:138878. https://doi.org/10.1016/j.scitotenv.2020.138878
Sicard P, De Marco A, Agathokleous E, Feng Z, Xu X, Paoletti E, Rodriguez JJD, Calatayud V (2020) Amplified ozone pollution in cities during the COVID-19 lockdown. Sci Total Environ 735:139542. https://doi.org/10.1016/j.scitotenv.2020.139542
Siciliano B, Dantas G, da Silva CM, Arbilla G (2020) Increased ozone levels during the COVID-19 lockdown: analysis for the city of Rio de Janeiro, Brazil. Sci Total Environ 737:139765. https://doi.org/10.1016/j.scitotenv.2020.139765
Singh V et al (2020) Diurnal and temporal changes in air pollution during COVID-19 strict lockdown over different regions of India. Environ Pollut 266:115368. https://doi.org/10.1016/j.envpol.2020.115368
Soni M, Verma S, Jethava P, Lamsal L, Gupta P, Singh J (2021) Impact of COVID-19 on the air quality over China and India using long-term (2009–2020) multi-satellite data. Aerosol Air Qual Res 21:200295. https://doi.org/10.4209/aaqr.2020.06.0295
Sulaymon ID et al (2021) COVID-19 pandemic in Wuhan: ambient air quality and the relationships between criteria air pollutants and meteorological variables before, during, and after lockdown. Atmos Res 250:105362. https://doi.org/10.1016/j.atmosres.2020.105362
Timsina J, Connor DJ (2001) Productivity and management of rice–wheat cropping systems: issues and challenges. Field Crops Res 69:93–132. https://doi.org/10.1016/S0378-4290(00)00143-X
Tong L et al (2017) Characteristics of surface ozone and nitrogen oxides at urban, suburban and rural sites in Ningbo, China. Atmos Res 187:57–68. https://doi.org/10.1016/j.atmosres.2016.12.006
Voulgarakis A, Wild O, Savage N, Carver G, Pyle J (2009) Clouds, photolysis and regional tropospheric ozone budgets. Atmos Chem Phys 9:8235–8246. https://doi.org/10.5194/acp-9-8235-2009
Wang L et al (2019) Observations of the atmospheric boundary layer structure over Beijing urban area during air pollution episodes. Atmos Chem Phys. https://doi.org/10.5194/acp-2018-1184
Wang H, Wang Y, Cai K, Zhu S, Zhang X, Chen L (2021) Evaluating the performance of ozone products derived from CrIS/NOAA20, AIRS/aqua and ERA5 reanalysis in the polar regions in 2020 using ground-based observations. Remote Sens 13:4375. https://doi.org/10.3390/rs13214375
Wild O, Zhu X, Prather M (2000) Fast-J: accurate simulation of in- and below-cloud photolysis in tropospheric chemical models. J Atmos Chem 37:245–282. https://doi.org/10.1023/A:1006415919030
Zhao Y et al (2020) Substantial changes in nitrogen dioxide and ozone after excluding meteorological impacts during the COVID-19 outbreak in Mainland China. Environ Sci Technol Lett 7:402–408. https://doi.org/10.1021/acs.estlett.0c00304
World Health Organization (2020) Guiding principles for immunization activities during the COVID-19 pandemic: interim guidance, 26 March 2020 (No. WHO/2019-nCoV/immunization_services/2020.1). World Health Organization

Publisher's Note Springer Nature remains neutral with regard to jurisdictional claims in published maps and institutional affiliations.

Springer Nature or its licensor holds exclusive rights to this article under a publishing agreement with the author(s) or other rightsholder(s); author self-archiving of the accepted manuscript version of this article is solely governed by the terms of such publishing agreement and applicable law.